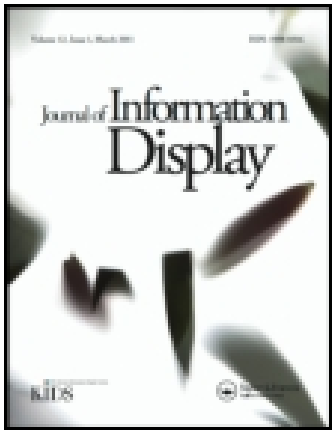

Journal of Information Display
Publication details, including instructions for authors and subscription information:
http://www.tandfonline.com/loi/tjid20

Low-temperature poly-silicon thin-film transistor developed without ion doping

C.M. Keum[a], J.K. Kim[a], S.J. Moon[a], S.K. Joo[b] & B.S. Bae[a]

[a] Department of Display Engineering, Hoseo University, Asan, Chungnam 336-795, South Korea

[b] School of Material Science and Engineering, Seoul National University, Seoul 151-742, South Korea

Published online: 20 Aug 2014.

To cite this article: C.M. Keum, J.K. Kim, S.J. Moon, S.K. Joo & B.S. Bae (2014) Low-temperature poly-silicon thin-film transistor developed without ion doping, Journal of Information Display, 15:3, 135-138, DOI: 10.1080/15980316.2014.950613

To link to this article: http://dx.doi.org/10.1080/15980316.2014.950613

Journal of Information Display, 2014
Vol. 15, No. 3, 135–138, http://dx.doi.org/10.1080/15980316.2014.950613

Taylor & Francis
Taylor & Francis Group

Low-temperature poly-silicon thin-film transistor developed without ion doping

C.M. Keum[a], J.K. Kim[a], S.J. Moon[a], S.K. Joo[b] and B.S. Bae[a*]

[a]*Department of Display Engineering, Hoseo University, Asan, Chungnam 336-795, South Korea;* [b]*School of Material Science and Engineering, Seoul National University, Seoul 151-742, South Korea*

(*Received 14 June 2014; accepted 24 July 2014*)

Low-temperature polycrystalline silicon (LTPS) thin-film transistors (TFTs) were developed without ion doping for lower cost. Aluminum (Al), a group 3 element, was used for the source and drain regions instead of ion doping. The effect of Al doping was verified through the Arrhenius plot to check the shift of the Fermi level. Al doping was applied for the metal-induced lateral crystallized polycrystalline silicon (Si) to achieve a p-channel LTPS TFT without ion doping. The TFT developed via Al doping exhibited 35.5 $cm^2/V\,s$ field effect mobility, a −3.7 V threshold voltage (V_{th}), a 4.0×10^5 on–off ratio, and a 0.7 V/dec subthreshold slope.

Keywords: thin-film transistor; doping; aluminum; polycrystalline silicon; display

Introduction

Thin-film transistors (TFTs) are currently being used widely in active-matrix displays and large-area electronics. The TFT technology is useful for high-resolution displays in combination with various display technologies, such as liquid crystal displays, electronic papers, organic light-emitting diodes, and other flat panel displays. The active-matrix organic light-emitting diode (AMOLED) has attracted much attention of late due to its low driving voltage, large viewing angle, and fast response time, and because it does not require a backlight. For AMOLED, low-temperature poly-silicon (LTPS) TFTs are being used instead of amorphous Si TFTs because the stability of the latter is worse than that of the former LTPS TFT [1,2] and because the LTPS TFTs have larger mobility than the amorphous Si TFTs. Due to the larger mobility of the LTPS TFTs compared with the amorphous Si TFTs, LTPS TFTs have advantages for displays, such as high-resolution, high-brightness, and high-speed images.

High-mobility LTPS TFTs are currently being used more in digital devices such as mobile phones, digital cameras, and AMOLED TVs [3,4]. In terms of high mobility, the amorphous oxide TFTs have attracted substantial attention in the display industry. In recent studies, amorphous In–Ga–Zn–O TFTs showed high mobility and a relatively simple process, but it is still not popular due to its low stability against bias illumination stress [5–8].

One drawback of the LTPS TFTs is their higher cost compared with amorphous Si TFTs. The LTPS TFT has additional processes compared with the amorphous Si TFT, such as crystallization and ion doping. Ion doping is used for the source and drain regions. The ordinary LTPS TFT uses ion doping with PH_3 or B_2H_6 as the doping gas for the N- and P-channel TFTs, respectively. Aluminum (Al) is a group 3 element in the periodic table that has three valence electrons [9,10]. When Al diffuses into Si, it replaces the Si atom and acts as an acceptor to generate a hole. Therefore, the Fermi level shifts down to the valence band edge, and the conduction activation energy decreases. There have been reports of the replacement of Si with Al for p-type doping [9], which showed p-channel TFTs with Al doping in the source and drain regions. Such studies, however, did not show the effect of Al doping on the Fermi level shift and, as such, the effect of Al doping on the Fermi level shift at various conditions was investigated in the present study. Also, Al doping was applied at a higher annealing temperature of 550°C, with metal-induced lateral crystallization (MILC) poly-Si. After the fabrication of the samples, the doping characteristics of Al and the transfer characteristics of LTPS TFTs were evaluated.

Experiment

LTPS TFTs with source and drain regions were developed via Al doping. Figure 1 shows the process flow of the LTPS TFT without ion doping. Pre-compaction was done at 600°C for 24 h to reduce the glass shrinkage and deformation. The thermal budget of the conventional furnace process is generally so high that the glass shrinkage may affect the TFT process on the glass substrate [10]. For the

*Corresponding author. Email: bsbae3@hoseo.edu

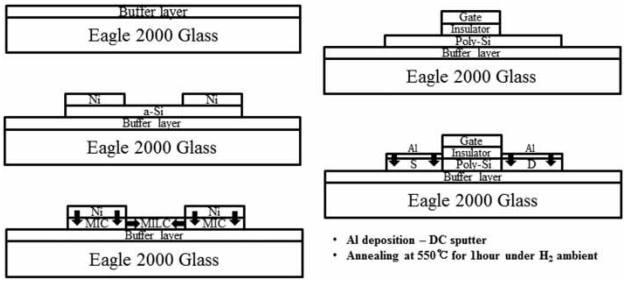

Figure 1. Process flow of the LTPS TFT without ion doping.

buffer layer, a 300-nm-thick SiO_2 layer was deposited on the glass via plasma-enhanced chemical vapor deposition (PECVD). Then a 100-nm-thick amorphous Si layer was deposited also via PECVD.

After the patterning of amorphous Si via reactive ion etching (RIE), it was crystallized via nickel-mediated MILC [11–15]. 0.5-nm-thick nickel was deposited via metal organic chemical vapor deposition. Crystallization was done at 550°C for 5 h, under a H_2 ambient in a tube furnace. For the gate insulator, 100-nm-thick Si oxide was deposited via PECVD. Then molybdenum–tungsten alloy (MoW) was sputtered as a gate metal. After gate pattern formation, the gate oxide was removed, except for the Si oxide under the gate electrode, via RIE with the SF_6, Ar, and CHF_3 gases. After the deposition of Al as thin as 5 nm to avoid electrical shortness between the source-drain and gate electrodes, it was annealed for 1 h at 550°C for Al doping. After etching, the Al was annealed for 2 h at 550°C at a H_2 ambient for source and drain activation and for the defect passivation of the dangling bond. The electrical properties were also measured at a dark box.

For the source and drain regions, Al doping is important and, as such, the Al doping conditions (e.g. annealing temperature and time) were optimized in this study. To check the electric conduction activation energy after Al doping, Al was deposited on a poly-Si layer via DC magnetron sputtering. The effects of the annealing temperature were investigated for the 350°C and 450°C annealing temperatures with the annealing time of 1 h. After annealing, the Al layer was removed with the Al etchant. The Al layer was again subjected to DC magnetron sputtering and was then patterned for the measurement of the electric conduction activation energy, as shown in the inset of Figure 2. The electrical conduction was measured for various temperatures, and the electrical conduction activation energy was obtained from the Arrhenius plot. With an optimized annealing temperature, the electrical conduction activation energies were measured for various annealing times to determine the optimized annealing time.

Results and discussion

The Fermi level shift through Al doping was extracted from the measurements of the electrical conductivity as a function of the temperature. As the doping concentration was increased, the Fermi level shifted to the valence band edge. The conduction activation energy, which is the energy difference between the valence band edge and the Fermi level, was obtained from the Arrhenius plot of the measured electrical conductivities.

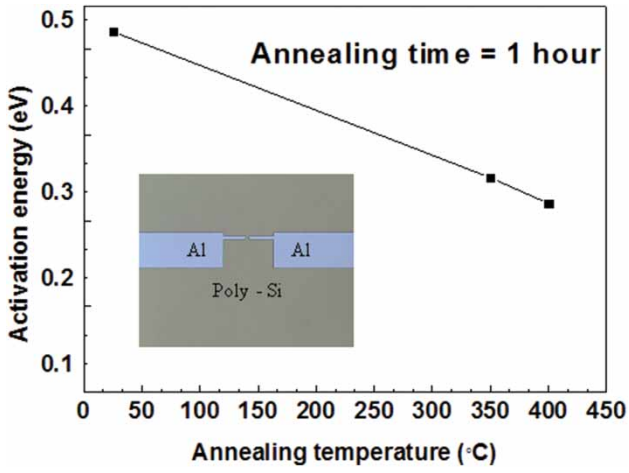

Figure 2. Electrical conduction activation energies according to the annealing temperatures.

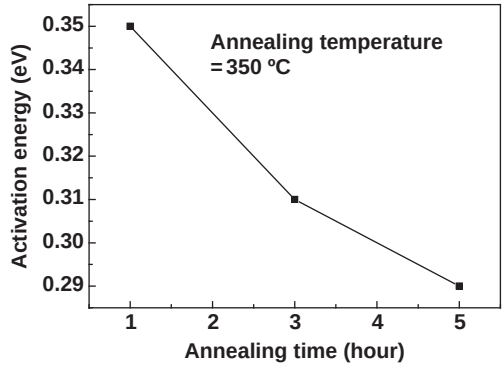

Figure 3. Electrical conduction activation energies for various annealing times.

Figure 2 shows the conduction activation energies according to the annealing temperature. The inset is a photograph of the electrodes. The conduction activation energy before annealing was 0.52 eV. When the annealing temperature was increased to 400°C, the conduction activation energy decreased to 0.32 eV. The lowered activation energy means that the Fermi level shifted to the valence band edge, which is the result of the Al doping through the replacement of the Si atoms.

Figure 3 shows the conduction activation energies for various annealing times at 350°C. For 1-h annealing, the activation energy was 0.35 eV; for 3-h annealing, 0.31 eV; and for 5-h annealing, 0.29 eV. Thus, as the annealing time was increased, the conduction activation energy decreased, and Al diffused to the Si and replaced the Si atom to become an acceptor.

Table 1. Activation energies of diffusion for various dopants (the quantity Q_A is referred to as the apparent activation energy of diffusion [15]).

Donor	Q_A (eV)
P	3.51, 3.61, 3.61, 3.66, 3.67
As	4.05, 4.08, 4.11, 4.23, 4.34
Sb	3.89, 3.98, 4.05
Bi	4.12
Acceptor	Q_A (eV)
B	3.25, 3.46, 3.50, 3.51, 3.87
Al	3.36
Ga	3.75
In	3.60

Table 1 contains data from many studies reported in the literature; these data are supposed to be valid for diffusions performed under intrinsic doping conditions. The quantity Q_A is referred to as the apparent activation energy of diffusion [15]. When boron was used as an acceptor, the activation energies were 3.25–3.87 eV, which were similar to that of the Al with 3.36 eV activation energy. In the case of poly-Si, the piped diffusion activation energy would be lower than that, and about 3.01 eV was reported for the piped diffusion of Al in Si [16]. The extracted conduction activation energies in this experiment decreased as the annealing temperature and time increased, which verified that Al was doped on the Si. Therefore, Al was used for source–drain doping instead of ion doping to develop a p-channel TFT. The p-channel LTPS TFT with Al-doped source and drain regions was evaluated.

The channel width and length of the fabricated LTPS TFT were 20 and 50 μm, respectively. Figure 4 shows the transfer characteristics of the fabricated LTPS TFT with Al-doped source and drain regions. The transfer characteristics show the typical p-channel TFT, which shows a large on-current at the negative gate voltages and a low off-current at the positive gate voltages. The low off-current for the positive gate voltages verified that the Al-doped source and drain regions were well doped as p-type. A further decrease in the off-current can be achieved through the use of additional structures such as an offset, a lightly doped drain (LDD), and dual or multiple gates.

In the case of Al doping, the control of the diffusion length of Al is one difficulty. As the annealing temperature becomes higher, the Al diffusivity increases. The lateral diffusion to the channel area decreases the effective channel length. Therefore, the controllability of the Al diffusion is one key hurdle to be overcome. The lateral diffusion of Al as an acceptor was reported as 2.5 μm/h at 400°C [9]. The annealing temperature for the source–drain in this experiment was 550°C, which enhanced the diffusion of Al compared with 400°C annealing. In Table 1, the activation energy for Al is 3.36 eV, but for the piped diffusion, it is lowered to 3.01 eV [17]. Based on this activation energy, the calculated ratio of diffusivity at 550–400°C is about 4. Therefore, the diffusion in this experiment was about four times faster than that at 400°C. From this result, it is expected that the lateral diffusion of Al is around 10 μm/h, which is about four times higher than 2.5 μm/h. Therefore, in the case of the 50 μm channel length, the effective channel length was expected to be about 30 μm through 10 μm subtractions at both the source and drain regions. Therefore, the source–drain resistance was expected to become ohmic in the case of the 20 μm channel length, which was verified by the measured transfer characteristics, as shown in Figure 5.

The transfer characteristics for the 20 μm channel length shown in Figure 5 verify a 10 μm/h or more diffusion. As shown in Figure 5, the diffusion of Al touched each source and drain region after Al doping annealing, and an ohmic channel between the source and drain regions was observed. Figure 6 shows the transfer characteristics for the

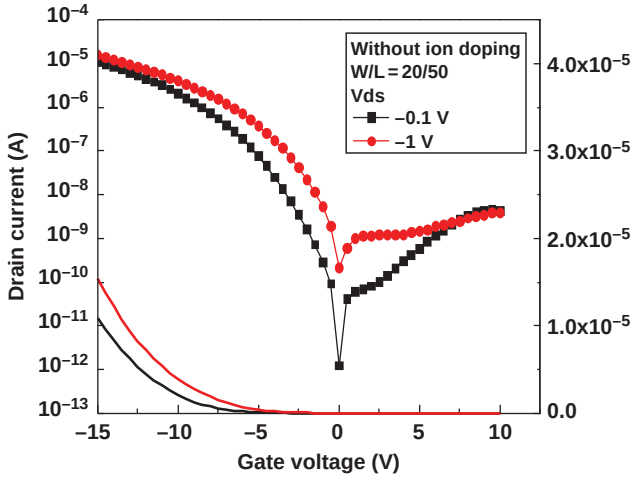

Figure 4. Transfer characteristics of the fabricated LTPS TFT without ion doping.

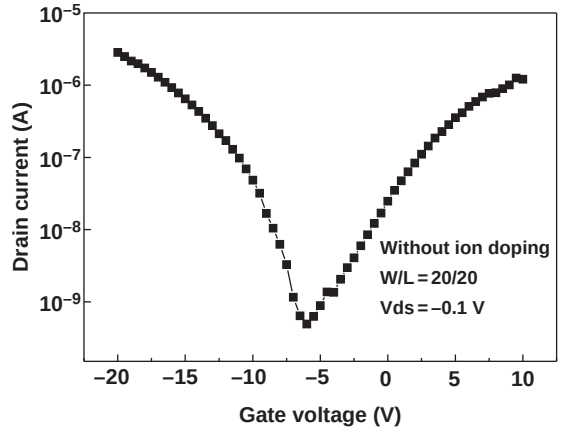

Figure 5. Transfer characteristics of the LTPS TFT with a 20 μm channel length.

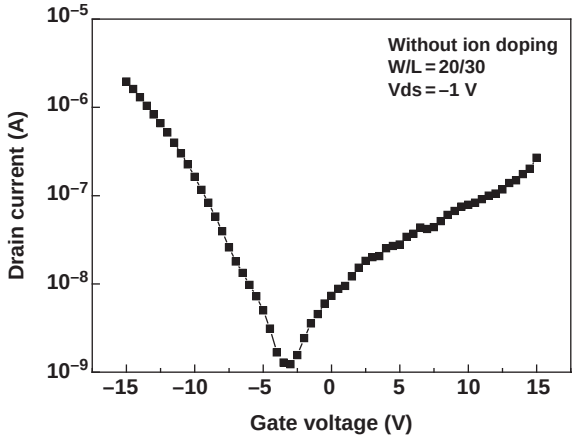

Figure 6. Transfer characteristics of the LTPS TFT without ion doping and with a 30 μm channel length.

Table 2. Electrical parameters of the fabricated LTPS TFT without ion doping.

W/L	25/30	20/50	20/30
V_{ds} (V)	−1	−0.1	−1.0
V_{th} (V)	−7.1	−5.4	−7.0
On-off ratio	5.2×10^6	2.3×10^2	1.4×10
On-current (A)	$4.0\times^{-5}$	8.1×10^{-8}	2.0×10^{-6}
SS (V/dec)	0.7	0.7	3.2
Mobility (cm^2/V s)	3.55×10^{-1}	3.99×10^{-5}	3.34×10^{-4}

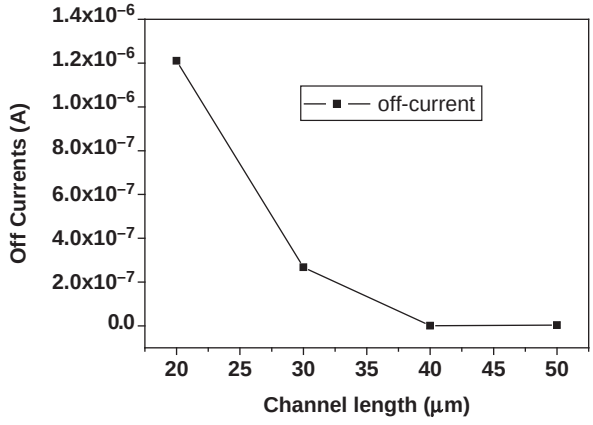

Figure 7. Channel length and off-current characteristics of the LTPS TFT.

30 μm channel length, where the current was drastically reduced compared with the 20 μm channel length. Therefore, 10 μm/h or slightly more diffusion was expected. As the channel length of the fabricated TFT was 50 μm, the effective channel length was expected to be 30 μm or slightly less. The parameters of the fabricated LTPS TFT without ion doping considering the effective channel length are given in Table 2.

Figure 7 shows the off-currents vs. channel lengths. For a shorter channel length such as 20 μm, the off-current was large due to the lateral diffusion of Al. As the channel lengths were increased, the off-current decreased. From the graph, the lateral diffusion was estimated to be 20–30 μm. Table 2 shows over 10^{-5} A on-currents and a 10^{-8} A off-current. To further reduce the off-current, an LDD or offset structure would be necessary.

Summary

The aluminum (Al) doping effect for various annealing temperatures and times was investigated. The Fermi-level shift was confirmed via the Arrhenius plot after Al doping. The conduction activation energy was decreased to 0.29 eV by Al doping. LTPS TFTs with Al doping were developed without ion shower doping. The fabricated TFTs showed p-channel TFT characteristics, which verified the source–drain doping by Al. A 4.0×10^5 on-off ratio, a 0.7 V/dec subthreshold slope, and 35.5 cm^2/V s field effect mobility were obtained for the fabricated TFTs with Al doping.

References

[1] S. Zhao, Z. Meng, W. Zhou, J. Ho, M. Wong, and H.S. Kwok, IEEE Trans. Electron Devices **6**, 1965 (2013).
[2] A. Mimura, G. Kawachi, T. Aoyama, and T. Suzuki, IEEE Trans. Electron Devices **3,** 513 (1993).
[3] T.-J. King, and K.C. Saraswat, IEEE Electron Dev. Lett. **13**, 309 (1992).
[4] J.H. Seo, Y.K. Park, Y.K. Koo, J. Heo, J.W. Park, and S.K. Joo, Electron Mater Lett. **1**, 309 (2006).
[5] K. Kato, Y. Shionoiri, Y. Sekine, K. Furutani, T. Hatano, T. Aoki, M. Sasaki, H. Tomatsu, J. Koyama, and S. Yamazak, Jpn. J. Appl. Phys. **51**, 021201 (2012).
[6] H. Ohshima, Jpn. J. Appl. Phys. **53**, 3S1 (2014).
[7] H.S. Shin, B.D. Ahn, Y.S. Rim, and H.J. Kim, J. Inf. Disp. **12**, 209 (2011).
[8] S.H. Kim, K.S. Jeong, G.W. Lee, and H.D. Lee, J. Inf. Disp. **14**, 61 (2013).
[9] D. Zhang, and M. Wong, IEEE Electron Dev. Lett. **27**, 564 (2006).
[10] M. Anma, J. Soc. Inf. Display **9**, 95 (2001).
[11] S.W. Lee, E.G. Kim, S.S. Han, H.S. Lee, D.C. Yun, K.M. Lim, M.S. Yang, and C.D. Kim, IEEE Electron Dev. Lett. **24**, 174 (2003).
[12] Z. Meng, M. Wang, and M. Wong, IEEE Trans. Electron Devices **47**, 404 (2000).
[13] D.L. Zhang, and M. Wong, J. Soc. Inf. Display **13**, 815 (2005).
[14] S.W. Lee, and S.K. Joo, IEEE Electron Dev. Lett. **74**, 160 (1996).
[15] P.M. Fahey, P.B. Griffin, and J.D. Plummer, Rev. Modern Phys. **68**, 289 (1989).
[16] L.K. Lam, S.K. Chen, and G. Dieter, App. Phys. Lett. **29**, 1866 (1999).
[17] D. Demirevay, and B. L¨ammelz, J. Phys. **30**, 1972 (1997).